Microsyst Technol (2016) 22:2185–2192
DOI 10.1007/s00542-015-2609-1

TECHNICAL PAPER

Low power highly sensitive platform for gas sensing application

Rahul Prajesh[1,2] · **Nishit Jain**[1] · **Ajay Agarwal**[1,2]

Received: 31 March 2015 / Accepted: 18 June 2015 / Published online: 1 July 2015
© Springer-Verlag Berlin Heidelberg 2015

Abstract This paper reports a low power miniaturized MEMS based integrated gas sensor with 36.84 % sensitivity ($\Delta R/R_0$) for as low as 4 ppm (NH_3) gas concentration. Micro-heater based gas sensor device presented here consumes very low power (360 °C at 98 mW/mm^2) with platinum (Pt) micro-heater. Low powered micro-heater is an essential component of the metal oxide based gas sensors which are portable and battery operated. These micro-heaters usually cover less than 5 % of the gas sensor chip area but they need to be thermally isolated from substrate, to reduce thermal losses. This paper elaborates on design aspects of micro fabricated low power gas sensor which includes 'membrane design' below the microheater; the 'cavity-to-active area ratio'; effect of silicon thickness below the silicon dioxide membrane; etc. using FEM simulations and experimentation. The key issues pertaining to process modules like fragile wafer handling after bulk micro-machining; lift-off of platinum and sensing films for the realization of heater, inter-digitated-electrodes (IDE) and sensing film are dealt with in detail. Low power platinum microheater achieving 700 °C at 267 mW/mm^2 are fabricated. Temperature calculations are based on experimentally calculated thermal coefficient of resistance (TCR) and IR imaging. Temperature uniformity and localized heating is verified with infrared imaging. Reliability tests of the heater device show their ruggedness and repeatability. Stable heater temperature with standard deviation (σ) of 0.015 obtained during continuous powering for an hour. Cyclic ON–OFF test on the device indicate the ruggedness of the micro-heater. High sensitivity of the device for was observed for ammonia (NH_3), resulting in 40 % response for ~4 ppm gas concentration at 230 °C operating temperature.

✉ Rahul Prajesh
rahulprajesh@gmail.com

Ajay Agarwal
dr.ajay123@gmail.com

[1] CSIR-Central Electronics Engineering Research Institute (CSIR-CEERI), Pilani 333031, Rajasthan, India

[2] Academy of Scientific and Innovative Research (AcSIR), New Delhi, India

1 Introduction

Miniaturized micro-heaters are needed for localized heating in gas sensing applications. Various gases respond to metal oxide based sensing films at elevated temperatures. For example, tin oxide (SnO_2) responds to NO_2 in the temperature range of 30–80 °C while NH_3 responds at higher temperature (250–300 °C) (Anothainart et al. 2003). These micro-heaters need to be small in size, stable at higher temperatures (~400 °C) and should consume low power. Attempts have been made for the optimization of micro-heater (Sheng 1998; Agbor 1997; Xu 2011; Lee 1996; Baroncini et al. 2004; Creemer et al. 2008; Hwang et al. 2011; Vereshchagina et al. 2015; Saxena 2013) platform for gas sensing application. To realize a reliable micro-heater platform for gas sensing applications, various materials, geometries and sizes have been considered. Membrane optimization (Rossi 1998) is an important task for fabricating a low power heater platform. Researchers have also tried silicon-on-insulator (SOI) wafer for fabricating a released gas sensor device (Laconte 2004). This paper presents various aspects of micro-heater design and its fabrication processes aimed at integrating these micro-heaters with interdigitated electrodes (IDE) and sensing film to make a complete gas sensor. A micro-heater based gas sensing platform with lower power consumption and fast thermal response time is needed for realizing a miniaturized gas sensor device. These microheaters should be able to provide uniform temperature as non-uniformity in temperature can lead to reduction in active sensing area and hence degradation of the sensor sensitivity and selectivity.

Micro heater design issues regarding heat dissipation to the whole sensor body because of closed membrane (Prajesh et al. 2014) have been dealt in detail in this work. Heat dissipation through body also complicates packaging requirements as such devices require thermally insulating packages, to reduce heat loss through package. These heater devices are also influenced by environmental conditions, in the absence of localized heating and thus the temperature stability of such micro-heater devices is poor. The presented work elaborates on process modules like (1) complete removal of silicon below the 1 µm thick silicon dioxide membrane which is integrated with micro-heater, IDE, sensing film and associated dielectric films, (2) metal/metal oxide lift-off for microheater, IDE and sensing film, and (3) processing of partially thinned fragile wafer. The work shows a reasonably low powered micro-heater based gas sensor device in contrast to the recent attempts (Vereshchagina et al. 2015). The presented micro-heater platform is integrated with interdigitated electrodes and tin oxide (SnO_2) to make a gas sensor device. Tin oxide is a multipurpose sensing film with various target applications (Anothainart et al. 2003; Prajesh et al. 2014; Moon et al. 2014; Pavelko et al. 2009; Tabata et al. 2005).

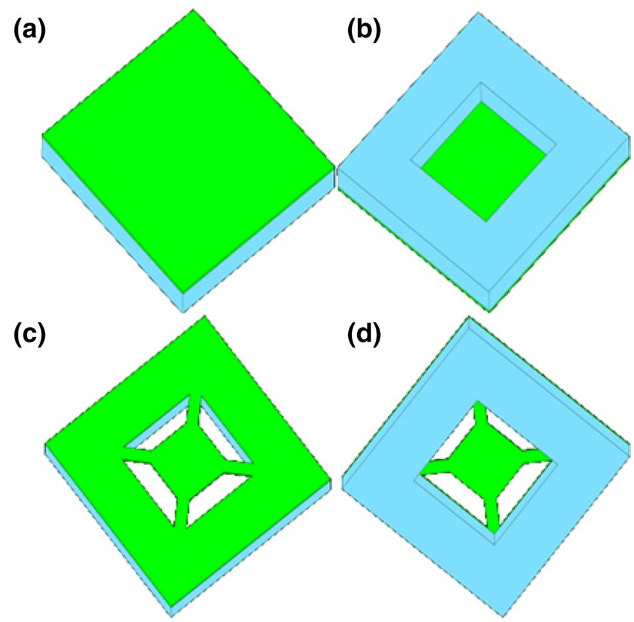

Fig. 1 Schematic view of two membrane types; closed membrane **a** top view, **b** bottom view and suspended membrane, **c** top view, **d** bottom view

2 Design considerations

2.1 Material selection

Various materials such as TiN (Creemer et al. 2008), platinum (Xu 2011; Baroncini et al. 2004; Prajesh et al. 2014; Xu 2012), and poly-silicon (Lee 1996; Hwang et al. 2011; Rossi 1998; Laconte 2004) are being used for the micro-heater application. Material selection depends on parameters such as thermal stability at operational temperature, chemical stability, cost, etc. A major portion of the micro-heater cost is attributed to its processing whereas only 10–15 % is due to the cost of material used. Platinum offers thermal stability at higher temperatures and its resistance remains stable even after large number of temperature cycles. Inertness of platinum in oxidizing ambient, even at elevated temperatures makes it one of the preferred materials for microheater applications regardless of the higher cost of platinum compared to other heater materials.

2.2 Suspended or closed membrane design

The power losses from the microheater to the chip surrounding can be reduced by designing the entire sensor device on a thin silicon dioxide membrane with no underneath silicon. Two types of membrane (Fig. 1) are considered for heater fabrication; closed membrane type and the suspended membrane type. Both the designs have their advantages and disadvantages. A suspended membrane has lesser connectivity to the bulk hence lesser thermal mass for lateral heat transfer, in-turn lesser power consumption compared to closed membrane. However, suspended membrane structures have lesser mechanical strength and are prone to damages due to shocks. An optimized close membrane can provide good mechanical strength and reasonable power consumption.

The complete gas sensor integration is comparatively difficult with suspended membrane type structure as the processes after releasing the membrane are stressful and releasing the membrane after complete device integration is equally challenging.

2.3 Silicon thickness under the silicon dioxide membrane

Membrane thickness below the micro-heater active area is an important parameter that needs optimization. It is important to remove entire silicon under the silicon dioxide membrane in order to achieve the optimized heating and cooling responses and lower power of the micro-heater. The effect of silicon thickness under the silicon dioxide membrane was analysed by controlled dry etching of silicon using SF_6. Micro-heater power and

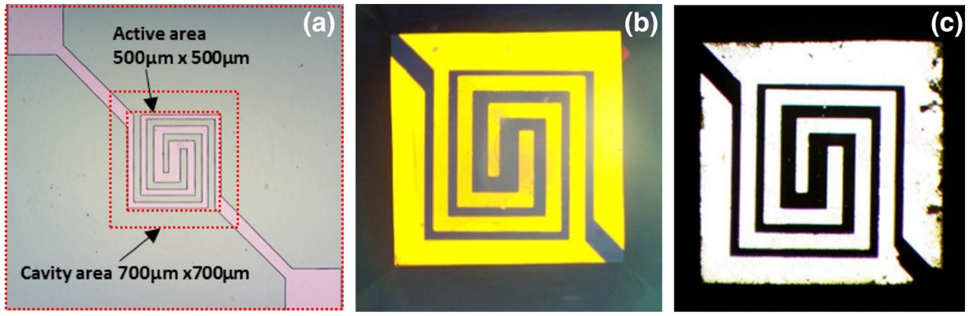

Fig. 2 **a** Microheater depicting the active (heater) area and cavity area; **b** released heater images with 3 µm thick silicon (partially transparent) and **c** no silicon (fully transparent) below the silicon dioxide membrane

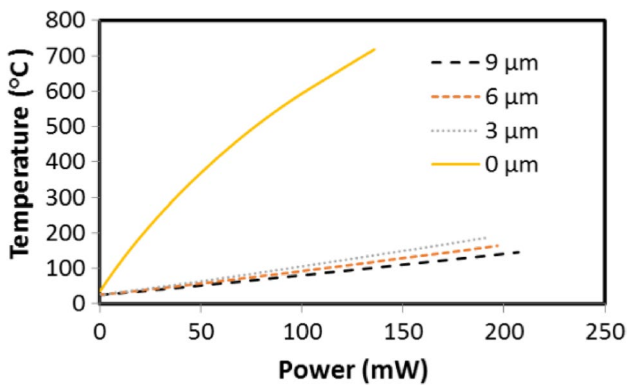

Fig. 3 Microheater power vs. temperature curve measured for four different silicon thicknesses under the 1 µm silicon dioxide membrane

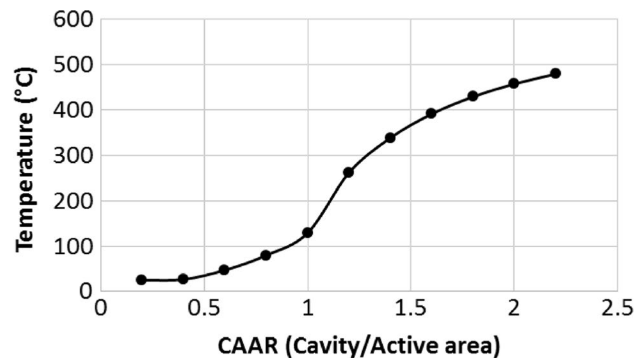

Fig. 4 FEM simulations for CAAR vs temperature showing sudden increase in temperature when CAAR in greater than 1

corresponding temperatures were recorded with varied silicon under the silicon dioxide membrane having active area 500 µm × 500 µm and cavity size of 700 µm × 700 µm (Fig. 2a). The measurements were carried out for silicon thicknesses 9, 6, 3 µm (Fig. 2b) and for device with no silicon left (Fig. 2c). At a given power, as the silicon thickness reduces the heater temperature increases. Once the silicon is completely removed, the temperature surges drastically (Fig. 3). Even <1 µm thick silicon under the silicon dioxide is undesirable as it leads to higher heat dissipation to the chip (Prajesh et al. 2014) leading to complexity in device packaging.

2.4 Cavity size

Another important design aspect for a micro-heater is the Cavity to Active Area Ratio (CAAR). The effect of CAAR has not been dealt in earlier works. The FEM simulation for different cavity sizes was carried out for obtaining temperature at different CAAR values. For simulation, the micro-heater (Fig. 2a) was modelled as having 0.2 µm thick platinum as heater element, and 1 µm silicon dioxide as electrical/thermal isolation between silicon substrate (50 µm) and heater element. The structure has an active are of 500 µm × 500 µm and cavity area was varied from 100 µm × 100 µm to 1100 µm × 1100 µm. The conduction, convection and radiation losses were considered and the device was sourced with a constant power at 0.5 V.

At first instance, it is clear from deduction of thermal losses that at given input power higher temperature is achieved when CAAR is more than one (Fig. 4). If CAAR is less than 1, the heater temperature reduces while keeping it close to 2 lead to poor mechanical stability of the device. Simulations also show that at CAAR value less than one, temperature is comparatively less and it increases drastically as CAAR increases beyond one.

3 Device fabrication

Device fabrication starts with the piranha cleaning (H_2SO_4:H_2O_2 = 5:1) of n-type ⟨100⟩ double side polished silicon wafers. Cleaned wafers were thermally oxidized in steaming oxygen to grow 1 µm SiO_2 layer which works as electrical and thermal insulating layer between micro-heater and silicon wafer and supports the entire microheater and sensor structures. First lithography for backside cavity opening was done on wafers followed by etching of SiO_2 in buffered HF. After oxide etching, bulk micromachining of the samples was done to remove the silicon from the backside in 25 % tetra-methyl-ammonium hydroxide (TMAH) solution with optimized silicon etch rate of 0.6 µm/min at 85 °C. Silicon etching was stopped to leave ~10 µm silicon.

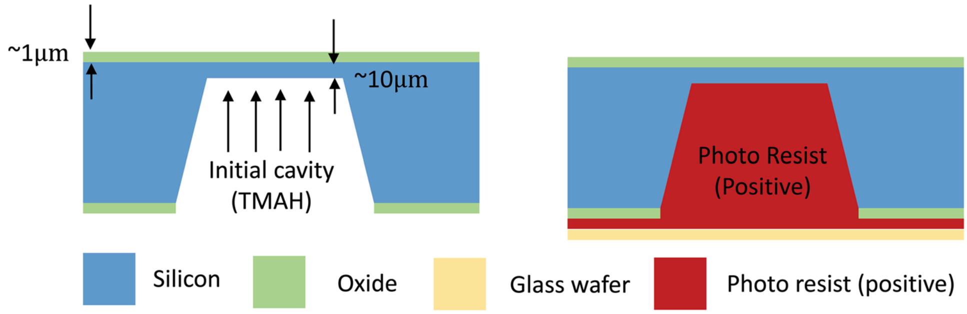

Fig. 5 Pictorial representation of the attachment of handle wafer for the handling of fragile wafer after bulk micromachining

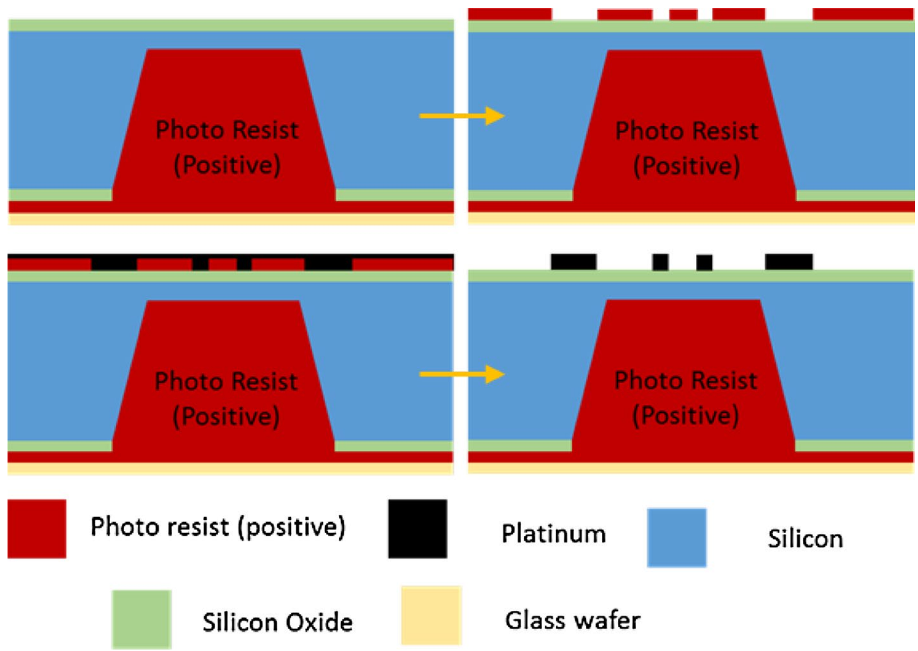

Fig. 6 Lift-off scheme followed during fabrication of gas sensor platform

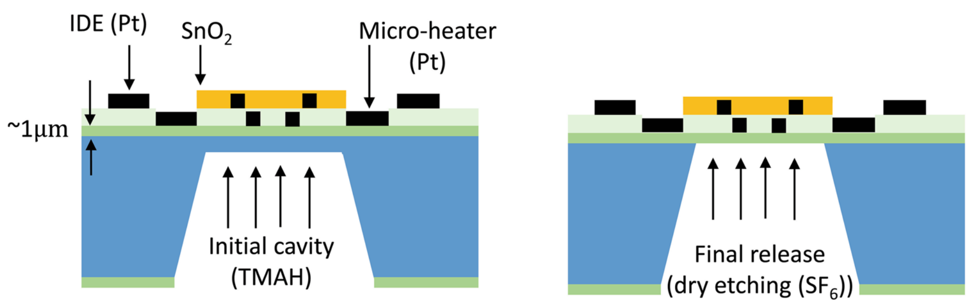

Fig. 7 Oxide membrane release module at the final stage of device fabrication

Such wafers face difficulty in further processing due to reduced mechanical strength, so wafers were bonded with handle glass wafers using photoresist (Fig. 5). The next photo lithography for heater patterning was done using dark field mask to realize platinum heater (varying line width in Fig. 2 is designed to achieve temperature uniformity) using lift-off process (Fig. 6). 20/200 nm Ti/Pt was deposited in a DC pulse sputtering system and liftoff was carried out in acetone. Handle wafers also get detached from process wafers in acetone during lift-off and they were bonded again after degreasing in tri-chloro-ethylene (TCE), acetone and isopropyl alcohol (IPA). 0.5 µm thick silicon nitride (PECVD) was then deposited to electrically isolate inter-digitated electrodes (IDE) and sensing film from the micro-heater followed by heater pad opening by lithography and dry etching of Si_3N_4. Photo lithography for IDE, 20/150 nm thick Ti/Pt deposition and lift-off was then completed. Inter digitated electrodes (IDE) were patterned to monitor the sensing film resistance during the gas exposure on the film. Finally, wafers were patterned for sensing film followed by

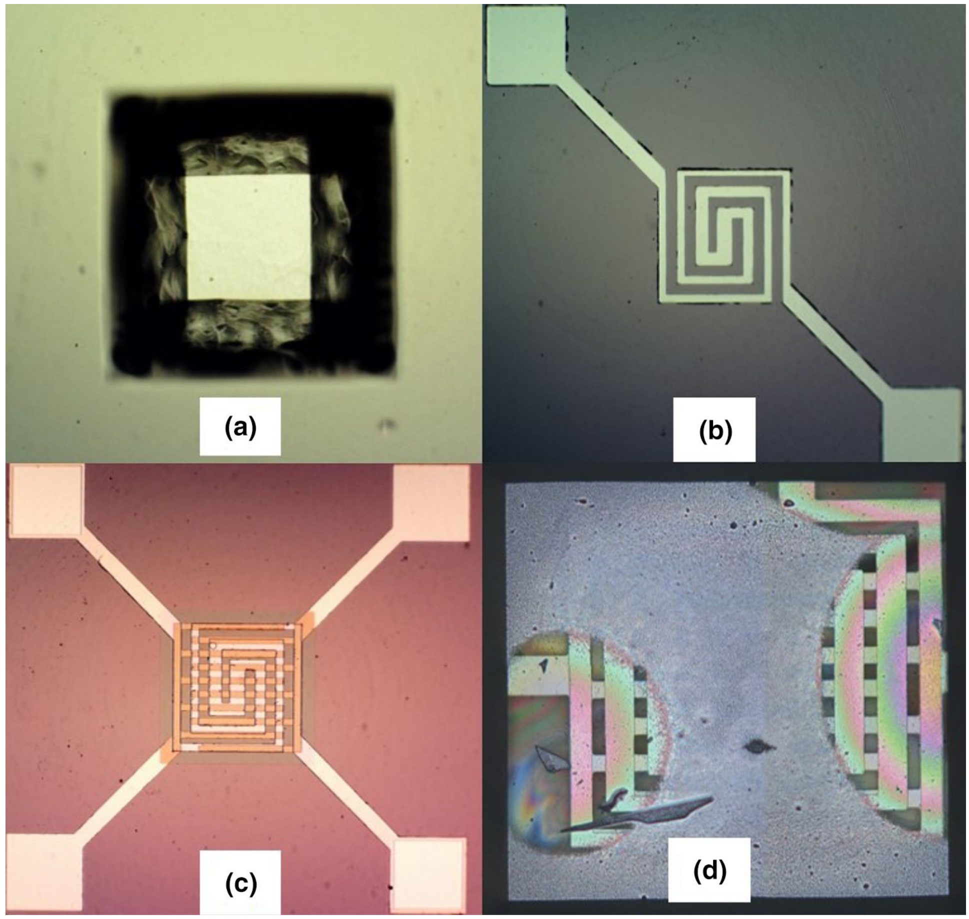

Fig. 8 Optical images of the device after some process steps during gas sensor fabrication. **a** silicon etching from backside (leaving ~ 10 µm silicon), **b** micro-heater geometry patterned on the front side after first lift-off process, **c** device after heater, IDE and sensing film realization and **d** intermediate step while removing last few microns of silicon from the backside of the wafer

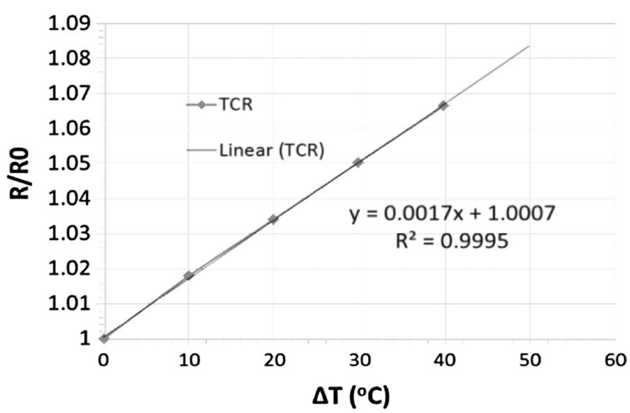

Fig. 9 Thermal coefficient of resistance (TCR) calculation using temperature vs resistance plot

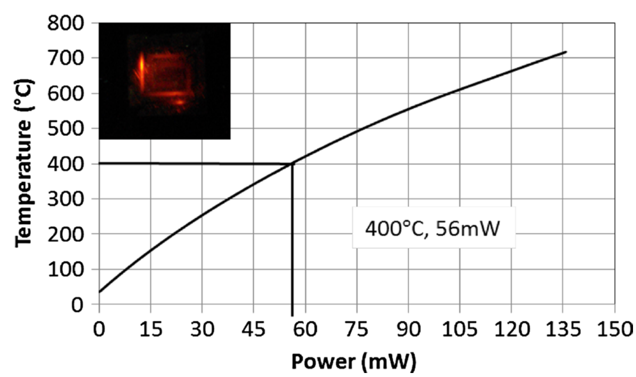

Fig. 10 Power vs temperature plot for micro-heater; giving 400 °C at 56 mW; the *inset* shows the evidence of ~ 700 °C temperature (at ~ 128 mW)

sensing film deposition and lift-off. Sensing film deposition was done using reactive DC sputtering technique with 60–40 % combination of N_2 and O_2 inside the chamber. This completed the gas sensor device integration. The remaining ~10 μm silicon from the backside of the wafer was removed using controlled dry etching in $SF_6 + O_2$ ambient as shown in Fig. 7. Intermediate stages of Device integration and membrane release process are shown in Fig. 8.

4 Results and discussion

The performance of the micro-heater is evaluated by various electrical characterizations namely thermal coefficient of resistance (TCR), change in resistance with applied power, temperature stability with time, etc. Resistance of the platinum heater was used to monitor and control its temperature. To calculate the thermal coefficient of

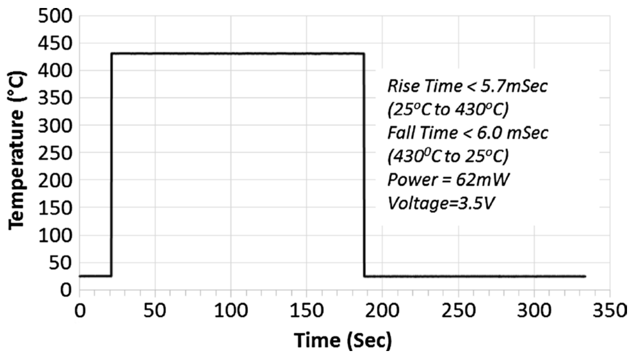

Fig. 11 Transient response of micro-heater indicates the rise time (25–430 °C) to be 5.7 ms and fall time (430–25 °C) as 6 ms

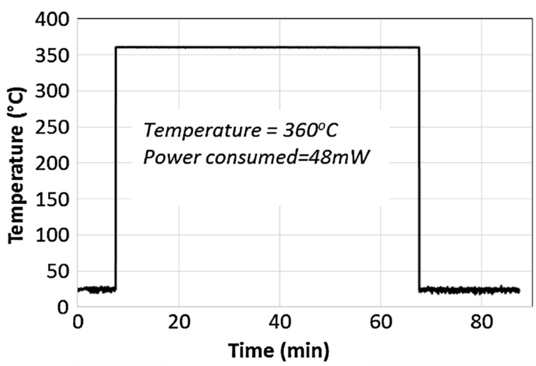

Fig. 12 Plot suggesting the stable temperature (360 ± 1 °C) when microheater was kept ON for 1 h

Table 1 Statistical analysis of the heater temperature when continuously heated for one hour as indicated in Fig. 11

Parameter	Value
Max	360.8702
Min	359.6443
Average	360.4755
Standard deviation	0.1585

resistance (TCR) value for the platinum, micro-heater pattern resistance was recorded at different temperatures by external heating. Figure 9 shows the curve which gives the TCR value (0.0017 °C^{-1}) as its slope. TCR value is then used for heater/sensor temperature calculations based on the change in the heater resistance. DC Voltage was applied on the micro-heater terminals to check the change in the heater resistance which can be converted to temperature using the formula given as

$$T = T_0 + (R - R_0)/(\alpha . R_0) \tag{1}$$

where R is the resistance at temperature T, α is the TCR value, R_0 is the resistance at temperature T_0 (room temperature). Figure 10 shows the temperature change with the applied power. A temperature of 400 °C is achieved at 56 mW power. The device was found to be stable up to a temperature 717 °C (Fig. 10). Evidence of a temperature close to 700 °C is given in Fig. 10 (inset). The power consumption in these heaters is significantly low thereby supporting their integration with the standard VLSI technology, to make a complete gas sensing solution on chip. Micro-heater's transient response was recorded as shown in Fig. 11 and the time to reach 430 °C from 25 °C was observed to be 5.7 ms whereas the fall time from 430–25 °C was recorded as 6 ms. The transient response shows that device responds rapidly. Reliability testing of the heater was done in two modes. Firstly, micro-heater was subjected to constant power for 1 h and heater temperature in the range of 360 ± 1 °C was observed (Fig. 12) with standard deviation of 0.1585 (Table 1). Another reliability test was carried out on device by applying ON/OFF cycles. 40 OFF/ON/OFF/ON cycles of 30/30/30/60 s were applied on the device to check the stability of the device during periodic forces (Fig. 13). Device temperature uniformity showing localized heating in the active area was also analyzed by infrared imaging (Fig. 14a, b).

Fig. 13 Micro-heater reliability testing with OFF/ON/OFF/ON (30/30/30/60 s) cycles

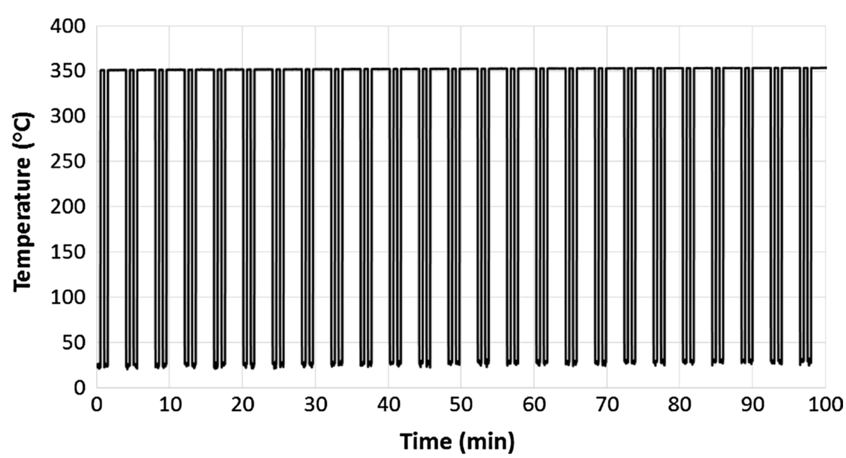

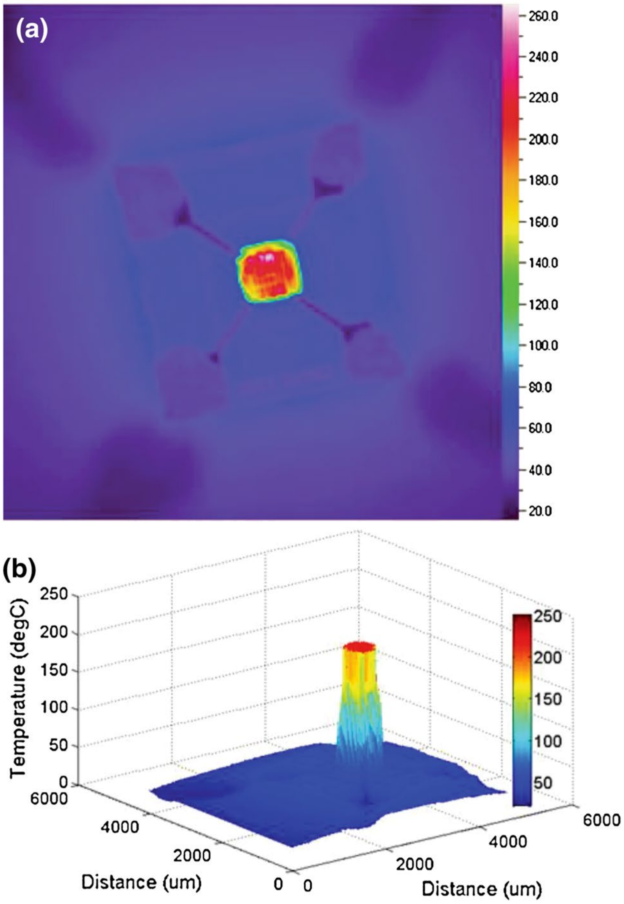

Fig. 14 Infrared imaging of the microheater showing uniform temperature. **a** ~ 220 °C in localized area; **b** corresponding 3D image

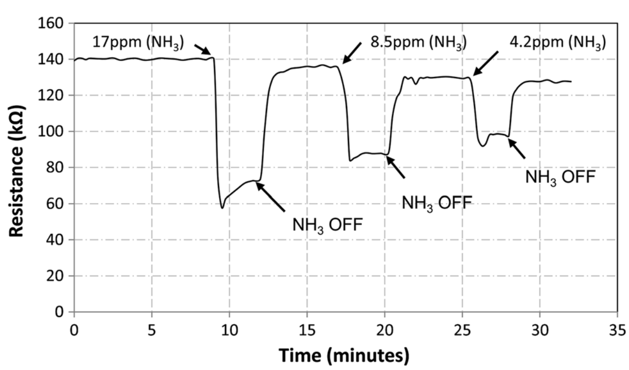

Fig. 15 Ammonia (NH_3) sensing response of the integrated gas sensor device: showing 17, 8.5 and ~4 ppm of ammonia gas in synthetic air

To ensure the application of the integrated device few gas sensing experiments were performed. A typical sensing measurement is reported in Fig. 15. The device was kept in a closed chamber for the measurement micro-heater was kept at 230 °C. Different gas concentrations can be easily distinguished with large individual response. For 100 ppm NH_3 a response of ~100 % ($\Delta R/R_{new}$) and ~40 % for ~4 ppm NH_3 was recorded. The gas concentration (ppm) was plotted (Fig. 16) with response, curve is quite linear and a linearity of ~0.999 was observed.

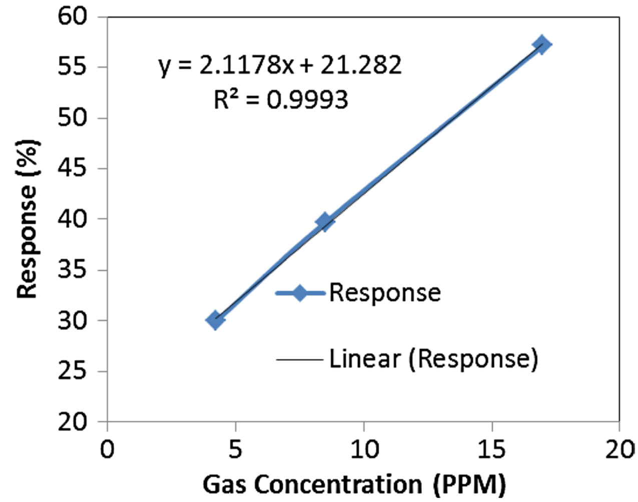

Fig. 16 Ammonia (NH_3) concentration vs sensing response curve, showing response linearity with gas concentration

5 Conclusions

The paper elaborated on various significant parameters for the design of micro-heater for gas sensing application. The micro-heater platform is highly reliable and consumes reasonably low power (114.3 mW/mm^2) at 400 °C. Device parameters such as silicon thickness below silicon dioxide membrane and cavity-to-active area ratio have been optimized. For low power devices and mechanical stability, it is highly suggested to have no silicon left below the silicon dioxide while cavity to active area ratio (CAAR) should be 1.5–2.0. Presented fabrication technique approach gives a broad insight for fabricating complete MEMS gas sensor device. Temperature uniformity across the device has been confirmed by Infrared imaging. Gas sensing response of the integrated device (with SnO_2 sensing film) for as low as 4.2 ppm NH_3 has been demonstrated. Response data shows a linearity of 0.999 with gas concentration.

Acknowledgments Authors would like to acknowledge Director, CSIR-CEERI for providing the infrastructure for the project and Head, MEMS and Microsensors group, for continuous encouragement. Authors also want to thank Dr. Vinay Gupta and his team for their constant technical support. Authors are also thankful to the technical staff of MEMS and Microsensors group, CSIR-CEERI for their wonderful support.

References

Agbor NE, Petty MC, Monkman AP (1997) An optical gas sensor based on polyaniline Langmuir-Blodgett films. Sens Actuators B Chem 41:137–141

Anothainart K et al (2003) Light enhanced NO_2 gas sensing with tin oxide at room temperature: conductance and work function measurements. Sens Actuators B Chem 93(1–3):580–584

Baroncini M et al (2004) Thermal characterization of a microheater for micromachined gas sensors. Sens Actuators B Chem 115(1):8–14

Creemer JF et al (2008) Microhotplates with TiN heaters. Sens Actuators A 148(2):416–421

Hwang WJ et al (2011) Development of micro-heaters with optimized temperature compensation design for gas sensors. Sensors (Basel) 11(3):2580–2591

Laconte J, Dupont C, Flandre D, Raskin JP (2004) SOI CMOS compatible low-power microheater optimization for the fabrication of smart gas sensors. IEEE Sens J 4(5):670–680

Lee DD, Chung WY, Choi MS, Baek JM (1996) Low-power micro gas sensor. Sens Actuators B Chem 33:147–150

Moon SE et al (2014) Low power consumption micro C2H5OH gas sensor based on micro-heater and ink jetting technique. Sens Actuators B Chem 217:146–150

Pavelko RG et al (2009) Comparative study of nanocrystalline SnO_2 materials for gas sensor application: thermal stability and catalytic activity. Sens Actuators B Chem 137(2):637–643

Prajesh R, Jain N, Khanna VK, Gupta V, Agarwal A (2014) MEMS based integrated gas sensor for NO_2 and NH_3. J ISSS 3(2):1–6

Rossi C, Temple-Boyer P, Esteve D (1998) Realization and performance of thin SiO_2/SiNx membrane for microheater applications. Sens Actuators A 64:241–245

Saxena G, Paily R (2013) Analytical modeling of square microhotplate for gas sensing application. IEEE Sens J 13(12):4851–4859

Sheng LY, Tang Z, Wu J, Chan PC, Sin JK (1998) A low-power CMOS compatible integrated gas sensor using maskless tin oxide sputtering. Sens Actuators B Chem 49:81–87

Tabata S et al (2005) A micromachined gas sensor based on a catalytic thick film/SnO_2 thin film bilayer and a thin film heater. Sens Actuators B Chem 109(2):190–193

Vereshchagina E et al (2015) Low power micro-calorimetric sensors for analysis of gaseous samples. Sens Actuators B Chem 206:772–787

Xu L, Li T, Gao X, Wang Y (2011) Development of a Reliable Micro-Hotplate with low power consumption. IEEE Sens J 11(4):913–919

Xu L, Li T, Gao X, Wang Y (2012) A high-performance three-dimensional microheater-based catalytic gas sensor. IEEE Electron Device Lett 33(2):284–286